EFDA–JET–CP(14)06/32

T. Wauters, A. Lyssoivan, D. Douai, S. Brezinsek, J. Ongena, M. Tripský, P. Abreu, D. Alegre, E. Belonohy, T. Blackman, V. Bobkov, K. Crombé, E. Delabie, A. Drenik, M. Graham, D. Hartmann, E. Joffrin, D. Kogut, E. Lerche, T. Loarer, P.L. Lomas, A. Manzanares, M.-L. Mayoral, I. Monakhov, J.-M. Noterdaeme, M. Oberkofler, V. Philipps, V. Plyusnin, G. Sergienko, D. Van Eester and JET EFDA contributors

ICRF Discharge Production for Ion Cyclotron Wall Conditioning on JET

ICRF Discharge Production for Ion Cyclotron Wall Conditioning on JET

T. Wauters[1], A. Lyssoivan[1], D. Douai[2], S. Brezinsek[3], J. Ongena[1], M. Tripský[1], P. Abreu[4], D. Alegre[5], E. Belonohy[6], T. Blackman[7], V. Bobkov[6], K. Crombé[1], E. Delabie[8], A. Drenik[9], M. Graham[7], D. Hartmann[10], E. Joffrin[2], D. Kogut[2], E. Lerche[1], T. Loarer[2], P.L. Lomas[7], A. Manzanares[5], M.-L. Mayoral[7], I. Monakhov[7], J.-M. Noterdaeme[6], M. Oberkofler[6], V. Philipps[3], V. Plyusnin[4], G. Sergienko[3], D. Van Eester[1] and JET EFDA contributors *

JET-EFDA, Culham Science Centre, OX14 3DB, Abingdon, UK

[1]Laboratory for Plasma Physics, ERM/KMS, 1000 Brussels, Belgium, TEC partner
[2]CEA, IRFM, F-13108 St-Paul-Lez-Durance, France
[3]FZJ, IEK-4 Plasmaphysik, 52425 Jülich, Germany, TEC partner
[4]IST, Instituto de Plasmas e Fusão nuclear, 1049-001 Lisboa, Portugal
[5]CIEMAT, Laboratorio Nacional de Fusión, 28040 Madrid, Spain
[6]Max-Planck-Institut für Plasmaphysik, 85748 Garching, Germany
7JET-EFDA, Culham Science Centre, Abingdon, OX14 3DB, UK
[8]DIFFER, Nieuwegein, The Netherlands
[9]Jožef Stefan Institute, 1000 Ljubljana, Slovenia
[10]Max-Planck-Institut für Plasmaphysik, 17491 Greifswald, German
** See annex of F. Romanelli et al, "Overview of JET Results", (25th IAEA Fusion Energy Conference, St Petersburg, Russia (2014)).*

Preprint of Paper to be submitted for publication in Proceedings of the
25th IAEA Fusion Energy Conference, St Petersburg, Russia
13th October 2014 - 18th October 2014

ABSTRACT

Discharge wall conditioning is an effective tool to improve plasma performance by (i) reducing the generation of plasma impurities liberated from the wall and (ii) controlling the recycling of hydrogenic fluxes. On ITER discharge wall conditioning will be employed as well for (iii) mitigating the tritium inventory build-up, for which one relies mostly on the removal of tritium-rich co-deposited layers. Ion cyclotron wall conditioning (ICWC) is a well-studied discharge wall conditioning technique having the advantage over Glow Discharge Conditioning (GDC) that it is applicable in the presence of magnetic fields. The ICWC mode of operation is included in the functional requirements of the ITER ion cyclotron resonance heating and current drive system, and is envisaged for use between ITER plasma pulses, in the presence of the toroidal magnetic field.

Ion Cyclotron Range of Frequencies (ICRF) plasma production employing ICRH&CD antennas designed for Fast Waves excitation is studied extensively on JET in the frame of fuel removal experiments by isotopic exchange aiming at the development of ICWC scenarios for ITER. This paper compares isotopic exchange efficiencies of JET ICWC discharges produced at ITER half and full field conditions for the JET carbon (C) and ITER like wall (ILW). ICWC on the ILW is found to be more efficient providing cleaner plasma faster, and has as significant advantage compared to the C-wall: an improved ratio of retained discharge gas to removed fuel, mitigating permanent retention during conditioning. A close to complete isotopic change over of the JET-ILW by D_2-ICWC alone, evidenced by sampling the plasma isotopic ratio in tokamak discharges, was achieved within 630s of cumulated ICWC discharge time. The accessible reservoir by H_2-ICWC at ITER half field conditions on the JET-ILW preloaded by D_2 tokamak operation is larger than 7.3×10^{22} hydrogenic atoms.

Conditioning efficiency optimization, ICRF discharge initiation and the characterization of the ICWC particle flux on the PFC are briefly addressed.

1. INTRODUCTION

Discharge wall conditioning in magnetic fusion devices is an effective tool to control fuel recycling and the influx of plasma impurities liberated from the plasma facing-components (PFC), and is generally used to provide reproducible discharge conditions and improved plasma performance [1]. On ITER, in addition to controlling the PFC surface state, the plasma isotopic ratio and easing plasma start-up, discharge wall conditioning will contribute to the mitigation of the tritium inventory build-up [2]. Ion cyclotron wall conditioning (ICWC) is based on low temperature ion cyclotron resonance (ICR) plasmas in reactive or noble gases, generated in tokamaks or stellarators in the presence of the toroidal magnetic field [1]. This is a key feature that allows wall conditioning during operational campaigns on superconducting fusion devices with permanent magnetic field, in contrast to Glow Discharge Conditioning (GDC) [2]. Therefore, ICWC is being developed for ITER as a baseline technique in which the ion cyclotron heating and current drive system will be employed to produce and sustain the conditioning plasma [3].

Recent experiments on JET assessed ICWC for isotope exchange on the ITER-like wall (ILW) equipped with a Be main chamber and a W divertor [4] and compared the efficiency to earlier experiments with the JET-CFC wall. This contribution presents an overview of these experiments with focus on (i) investigating the accessible fuel reservoir and comparing the ICWC efficiency between JET-CFC vs. JET-ILW, ITER full field vs. half field scenario, and operation with different vacuum pumping speeds, (ii) ICRF discharge production on JET and (iii) characterization of the wall conditioning fluxes.

2. EXPERIMENTAL SETUP

The use of ICWC during the non-active operation phase (H plasmas) and active phase (D and D:T plasmas) of ITER implies fixed toroidal field values of respectively half (B_0 = 2.65T) and full (5.3T) nominal magnetic field. Operating the JET antennas at 25MHz with toroidal field values of respectively B_0 = 3.3T and 1.65T simulates on JET the ITER full (5.3T/40MHz) and half (2.65T/40MHz) field case with on axis location of fundamental D^+ (resp. H^+) resonance layer. A small vertical magnetic field with field lines following the curvature of the inner and outer main chamber PFC is applied with amplitude optimized for maximal poloidal homogeneity ($B_V/B_0 = 8x10^{-3}$) [5].

Four separate JET experiments were performed: (i) ITER full field D_2-ICWC^{I} with cryo-pumping on H_2-GDC preloaded C-wall, (ii) ITER full field D_2-ICWC^{II} with turbo-pumping on H_2-GDC preloaded ILW, (iii) ITER half field H_2-ICWC^{III} with turbo-pumping on naturally D_2 preloaded ILW and (iv) ITER half and full field D_2-ICWC^{IV} with cryo-pumping on naturally H_2 preloaded ILW. Throughout the text the experiments are labelled by superscripts $^{I, II, III, IV}$ for clarity. The JET A2 antennas operated in plasma production mode with monopole phasing, coupling 50 to 300kW to low density ICRF plasma 0.3-5.0 $x10^{17}m^{-2}$. The discharge neutral pressures was controlled to values of 0.3-7.5 $x10^{-5}$mbar, typically via pre-programmed gas injection while experiment ICWC^{IV} benefitted from real time controlled gas injection rates keeping the neutral pressure close to the desired set value. Table 1 summarizes the discharge parameters.

Particle balances are obtained via (i) pressure recordings in the gas injection modules, (ii) residual gas analysis using (iia) pulse based mass spectrometry and penning gauge spectroscopy in ducts connected to the divertor, and (iib) volumetric analysis and relative composition analysis by gas chromatography of the total pumped gas after each of the experiments^{I,II,III}. The particle balance analysis for experiment ICWC^{IV} is ongoing. The evolution of the wall isotopic ratio is indirectly monitored via the plasma isotopic ratio from characteristic Balmer-beta radiation of H and D in the low temperature plasma.

3. COMPLETE ISOTOPE CHANGE OVER BY ICWC

Isotope exchange conditioning discharges aim at replacing hydrogen isotopes stored in the near surface (< 100 nm), which is required to control the plasma isotopic ratio of tokamak discharges. The isotopic exchange efficiency is expressed as the rate at which a technique can change the

isotopic ratio of the walls and the total extra retention it causes. Isotopic exchange experiments on JET are especially motivated by the need for assessing the exchange efficiency on the JET-ILW as well as JET's unique possibility to simulate D_2-ICWC in ITER full field conditions. Long-term fuel retention in JET operation with JET-ILW was already shown to be at least ten times lower than in JET-C whereas the accessible reservoir near the surface, reflected in the short-term retention, is expected to be in the same range [6].

Figure 1 (left axis) reflects the progressing change-over of the wall isotopic ratio via the plasma isotopic ratio obtained from H and D Balmer-beta radiation spectra along a vertical viewing line looking into the divertor measured by the same diagnostic for all 4 sets of pulses. A clear difference between JET-C^{I} and JET-$ILW^{II,III,IV}$ pulses is the lower initial *plasma* isotopic ratio.

The initial *wall* isotopic ratio as sampled by D_2-tokamak discharges after wall pre-loading for JET-ILW^{III} experiment is less than 2% on the figure scale. As the same vacuum pumping set-up was used (using cryo-pumps) both in the JET-C^{I} and JET-ILW^{IV} pulses, the plasma facing components are concluded to be the main cause for this difference, e.g. via a higher wall isotope release yield (~5 times) on JET-C^{I} wall compared to JET-$ILW^{II,III,IV}$. The wall preloading procedure for D_2-ICWC on JET-C^{I} and JET-ILW^{II} consisted of GDC, while for H_2-$ICWC^{III}$ and D_2-$ICWC^{IV}$ on the JET-ILW the wall was loaded by plasma operation.

Figure 1 (right axis), plotting the cumulated sum of the removed wall isotopes as a function of the total RF time, integrating each time over discharge and post discharge up to the start of the next pulse, illustrates that the removal (evacuated by pumps) is about two times faster for JET-$ILW^{II,III}$ than for JET-C^{I} (see as well Table 1). The analysis for experiment $ICWC^{IV}$ is ongoing. The supposed higher yield (release of wall isotopes per impinging plasma isotope) for JET-C^{I} is counter balanced by the poor ratio of net retention over removal. No clear difference for D_2-$ICWC^{II}$ at full field and H_2-$ICWC^{III}$ at half field appears from these results.

Although the plasma isotopic ratio remains stable after ~ 60s of discharge time (left axis), the cumulated amount of pumped wall isotopes shows no sign of saturation yet (right axis). The accessible fuel reservoir is clearly larger than the removal achieved within $206s^{III}$. The tendency of the latter H_2-$ICWC^{III}$ curve suggests that the limits of efficient wall isotope removal may become clearer upon at least doubling the total discharge time. Recently indeed, a close to complete change over was achieved after 630s of cumulated discharge time by D_2-$ICWC^{IV}$. Starting from an initial plasma isotopic ratio of 2%D, sampled by Balmer-beta radiation of H and D along a vertical line of sight looking into the divertor in the H_2 tokamak discharge preceding the D_2-$ICWC^{IV}$ pulses, the 630sec of D_2-ICWC resulted in a final plasma isotopic ratio of 95%D, sampled by D_2 tokamak discharges. This result proves that ICWC in ITER relevant f/B scenarios can effectively control the wall isotopic ratio of ITER like PFC's, within short (~600sec) total discharge time. It indicates as well that ICWC interacts with the PFC surfaces that dominate the recycling in tokamak plasmas (ref. [7]).

Table 1 summarizes the particle balances as obtained from gas injection data and chromatography analysis of the total pumped amount of gas. Within the limited number of RF pulses for D_2-$ICWC^{I}$

on JET-C it was possible to remove $1.6x10^{22}$ hydrogen particles (= about 6 monolayers) from the GDC preloaded wall, corresponding to approximately 10% of the short-term retention in JET-C accessible by plasma operation ($2x10^{23}$ atoms, [8]). For JET-ILW, thought to have a smaller accessible fuel reservoir in tokamak discharges than JET-C ($<1x10^{23}$ atoms [9]), D_2-ICWC^{II} on the H_2-GDC preloaded wall removed $2.9\ x10^{22}$ H atoms within a similar total RF discharge time. On increasing the later RF discharge time to 206s, for H_2-ICWC^{III} on JET-ILW, the amount of recovered atoms from the naturally loaded wall increases accordingly to $6.2x10^{22}$ D atoms, approaching complete depletion of the wall loaded hydrogen isotope. No/limited extra wall retention is observed in the JET-ILW pulses (last row of Table 1), whereas retention was about 3 times larger than removal in JET-C. The detailed particle balance analysis for ICWC^{IV} is ongoing.

The efficiency dependency for isotope exchange on discharge parameters, pressure, power and pulse length are studied in detail in [10]. It was found that for D_2 and H_2-ICWC on the JET-ILW^{II,III} the removal is strongly dependent on the loaded wall isotope concentration, significantly changing from pulse to pulse, as well as on the discharge duration (linear correlation coefficient R = 0.87 and 0.86 for resp. D_2^{II} and H_2^{III}-ICWC). For the JET-C^{I} pulses with constant pulse length and limited wall isotope depletion the dependency is largely determined by the coupled power (R = 0.90). Figure 2 plots the removed amount of wall isotopes as function of the product of coupled RF power P, pulse length Δt and wall isotope concentration N_w, reflecting the simple relation $dN_w/dt = f(P,p,\ldots)N_w$. The basic regression analysis allows estimating the accessible fuel reservoir by ICWC for both the JET-C and JET-ILW. Each of the plots assumes an initial accessible wall isotope concentration aiming at obtaining a satisfactory fit correlation above 85%. For (i) JET-C^{I} this requires setting the total amount of removed wall isotopes *lower* than 25% of the initial concentration. In (ii) the D_2-ICWC^{II} experiment *more* than 67% of the initial H on JET-ILW should be removed, while for (iii) the H_2-ICWC^{III} pulses on JET-ILW the optimal correlation is 0.85 when assuming that 85% of the initial D is removed. Table 2 summarizes the estimated values. While the particle balance analysis for the D_2-ICWC^{IV} experiment on the JET-ILW is ongoing, the close to complete changeover of the wall isotopic ratio illustrates already that the accessible fuel reservoir by ICWC is sufficiently large to control the isotopic ratio in tokamak plasmas.

4. ICRF PLASMA PRODUCTION

Conventional Ion Cyclotron Range of Frequencies (ICRF) antennas with poloidal current straps are designed and optimized for heating of dense target plasmas via excitation of Fast Waves (FW) with high coupling efficiency. Neutral gas breakdown with these standard poloidal ICRF antennas results from the acceleration of free electrons in the near antenna electrostatic vacuum parallel electric field ($E_{//}$) up to the ionization energy and subsequent electron-impact avalanche ionization. Upon reaching densities well above cut-off's for RF wave propagation the plasma is predominantly sustained by non-localised collisional absorption of RF power by electrons and ions [11].

The RF E//-field in vacuum is induced electrostatically from the RF potential difference between

the central conductor and the side parts of the antenna box (and side protection RF limiters), and inductively from the RF voltage induced between the tilted rods of the Faraday shield by the time-varying magnetic flux [12]. The field, which is non propagative in vacuum in present-size fusion devices due to the large toroidal wavelength at the typical ICRF band (~ 20−60MHz), decays both radially and toroidally. Phasing the antenna straps in monopole results in longer decay lengths and consequently in a wider radial area in vicinity of the antenna that participates in the initial avalanche like electron multiplication [12]. Plasma production has been extensively studied using single particle descriptions and basic analytic models. Recently a Monte Carlo approach was adopted for ICRF breakdown simulations (Code RFdinity1D [13]). The self-consistent model calculates electron trajectories in the magnetized torus, considering electron acceleration by the ICRF E//-field and electron-neutral and Coulomb collisions. The simulations confirm that the initial density build-up occurs mainly along magnetic field lines that pass in the close vicinity of the antenna area where the parallel electric field is high and additionally reveals that passing electrons, i.e. electrons encircling the torus while accelerating/decelerating on each passage through the antenna area, play a key role in the plasma formation. This is both the case for monopole and dipole antenna strap phasing as is clear from Figure 3. The figure shows the toroidal distribution of ionization events for an ICRF antenna located at toroidal position z = 0m. Ionization events are more frequent outside of the antenna area as the electric field tends to expel electrons from the antenna region. Secondly it can be seen that the ionization events outside the antenna area are distributed uniformly around the torus.

Experimental evidence for the initial plasma production at the low field side (LFS) was obtained via fast camera images recording the breakdown phase of H_2 ICRF discharges (Figure 4). The images show formation of a localized radiation zone at the LFS where after rapid plasma expansion over 3ms is observed towards the high field side (HFS). Two mechanisms are presently considered for the rapid expansion from LFS to HFS: (i) plasma formation driven by local excitation of plasma waves, where after propagation of the RF electric field causes further space ionization, and (ii) plasma expansion governed by charged particle transport across the toroidal magnetic field. The latter hypothesis, tested with the 1D (radial) transport code *Tomator1D*, requires coefficients well above (~10^3) those described by Bohm diffusion. To further establish the mechanisms of the different plasma production stages, dedicated codes focussing each on separate discharge phases [13-15] are being developed and integrated.

5. CHARACTERIZATION OF CONDITIONING FLUX

Fundamental in the study of discharge wall conditioning techniques is characterizing the particle fluxes to the vessel first wall. Although the standard diagnostic tools in present devices are not well adapted to low density and low temperature ICWC plasma, it was shown that 0D plasma modelling could be used successfully to retrieve insight on low energy wall flux components [14, 16]. The TOMATOR plasma simulator [14] is used to solve 0D energy and particle balance equations for hydrogen atomic and molecular plasma species, taking into account (1) elementary atomic and

molecular collision processes, (2) RF heating of electrons and protons, (3) particle and energy confinement, as well as (4) wall flux recycling, active pumping and gas injection.

Simulated for JET-ILW H_2-ICWC[III] pulses, one distinguishes (i) a low energy hydrogen atom flux of 1 to 5 x10^{20}/m^2s with energies between 3 and 5eV determined by Franck Condon energy upon dissociation and increased by elastic collisions with ions, and (ii) a low energy (atomic) hydrogen ion flux of 0.5 to 2.5 × 10^{19}/m^2s. It is expected that the high neutral flux enhances surface recombination and hence wall desorption. As neutrals are not constrained by the magnetic field, the neutral flux can be considered homogeneous, reaching also remote areas. For the ion flux it was shown that sheaths affect the ion impact energy on the wall to about 10–50eV [16]. As ions are transported along the magnetic field lines, the ion flux on JET is likely inhomogeneous, being highest on first limiting surfaces such as antenna protection limiters and inner bumpers. On ITER, designed with a shaped first wall, the ICWC ion-wetted area may approach the total surface area.

A third wall flux component consists of (iii) energetic neutrals stemming from CX reactions with the minor energetic plasma ion population (> 1keV) produced by resonant ICRF absorption, and evidenced by NPA diagnostic. The fast CX flux measured on JET is of the order of 1 × 10^{15} to 1 × 10^{17}/m^2s with Maxwellian energies of 1 to 10keV. While the high CX flux energies are sufficient to reach deeper surface layers and to cause physical sputtering, the flux was shown previously to have limited conditioning contribution in JET isotopic exchange ICWC discharges [17]. Energetic ion species produced by local resonant absorption are not described in the 0D plasma model.

Finally, (iv) as well an apparant warm ion component (80–160eV) was detected in the pulse averaged and instrument function corrected Doppler broadened H_α radiation spectra of discharges that featured highest energetic CX fluxes (Figure 5). This component, outside of the measurement range of the NPA diagnostic, and having at present a small signal to noise ratio in measured spectra requires further investigation. Quantifying the separate Hα emission sources requires study of H_2 dissociation and H excitation reaction rates for the cold component and H-ion CX collisions for the warm component with the Tomator code.

6. DISCUSSION AND CONCLUSIONS

JET ICWC discharges, reliably produced at ITER half[III,IV] and full field [I,II,IV] conditions, have shown their ability to change the wall isotopic ratio of JET-C[I] and JET-ILW [II,III,IV] within a limited number of discharges. A close to complete isotopic change over of the JET-ILW by D_2-ICWC alone was achieved within 630s of cumulated ICWC discharge time, and evidenced by sampling the plasma isotopic ratio in tokamak discharges. Besides the improved ICWC isotope exchange rate on the ILW[II,III] providing a cleaner plasma faster, a main advantage compared to CFC[I] is a reduction of the ratio of retained discharge gas to removed fuel, equal to ~ 3 for C-wall[I] and 0.86–1.4 for the ILW[II,III]. For maximizing the wall isotope removal per ICWC discharge one has to aim at long pulses with high (but still safe) RF power. As most of the isotopes are recovered in the post discharge phase (high outgassing pressure peak followed by slow pressure decay (See e.g. [18]), duty cycle

optimization studies for ICWC on JET-ILW still need further consideration.

The accessible fuel reservoir by H_2-ICWC on JET-ILW[III] preloaded by D_2 tokamak operation is found to be larger than $7.3x10^{22}$ hydrogenic atoms. This number is already ~ 2x larger than presently achieved in isotope exchange experiments by limiter plasmas [9]. The high removal without net retention on JET-ILW indicate that the ICWC wall fluxes in the presented experiments[II,III] feature inefficient beryllium erosion and redeposition in contrast to limiter plasmas [9]. The fuel inventory in beryllium deposits, predominantly located on main wall and at the top of the inner divertor [19], may be accessed. The possibility of complementing limiter plasmas with ICWC for fuel recovery after D:T pulses on ITER requires further investigation.

ACKNOWLEDGEMENTS

This work was supported by EURATOM and carried out within the framework of the European Fusion Development Agreement. The views and opinions expressed herein do not necessarily reflect those of the European Commission.

REFERENCES

[1]. J.Winter, Plasma Physics and Controlled Fusion **38** (1996)1503.
[2]. D. Douai et al., Proceedings of the 21st PSI, Kanazawa, Japan, 2014, submitted to Journal of Nuclear Materials.
[3]. ITER Project_Requirements_(PR)_27ZRW8_v4_6, (2010).
[4]. M Matthews et al, Journal of Nuclear Materials **438** (2013) S2–S10
[5]. D Douai et al, Journal of Nuclear Materials **415** (2011) S1021–S1028
[6]. S Brezinsek et al, Nuclear Fusion **53** (2013) 083023 (13pp)
[7]. S. Brezinsek and JET-EFDA contributors, 21st Int. Conference on Plasma Surface Interactions, Japan, May 2014
[8]. T. Loarer et al, Journal of Nuclear Materials **337–339** (2005) 624-628
[9]. T. Loarer et al, Proceedings of the 21st PSI, Kanazawa, Japan, 2014, submitted to Journal of Nuclear Materials
[10]. T. Wauters et al., Proceedings of the 21st PSI, Kanazawa, Japan, 2014, submitted to Journal of Nuclear Materials
[11]. A. Lyssoivan et al., AIP Conference Proceedings **1580** (2014) 287.
[12] A. Lyssoivan et al, Plasma Physics and Controlled Fusion **54** (2012) 074014
[13] M. Tripsky et al., 41st Conference on Plasma Physics, Berlin, Germany, June 2014.
[14]. T. Wauters et al., Plasma Physics and Controlled Fusion **53** (2011) 125003.
[15]. D. Van Eester et al., Plasma Physics and Controlled Fusion **35** (1993) 1189.
[16]. S. Möller et al, Proceedings of the 21st PSI, Kanazawa, Japan, 2014, submitted to Journal of Nuclear Materials
[17]. T. Wauters, Ghent University, publication 1978443 (2011), PhD Thesis
[18]. T. Wauters et al, Nuclear Fusion **53** (2013) 123001 (6pp)
[19]. A. Widdowson et al, Physica Scripta **T159** (2014) 014010

	JET-C D_2-ICWC^{I} 3.3T – 25MHz	JET-ILW D_2-ICWC^{II} 3.3T – 25MHz	JET-ILW H_2-ICWC^{III} 1.65T – 25MHz	JET-ILW D_2-ICWC^{IV} 1.65 & 3.3T 25MHz
Vacuum pumping	Cryopumps	Turbopumps	Turbopumps	Cryopumps
Wall preloading	H_2-GDC	H_2-GDC	D_2 plasma op.	H_2 plasma op.
Pressure [x10^{-5}mbar]	1.3 – 1.6	0.3 – 2.5	1.4 – 7.5	0.5 – 6.0
ICRF coup. power [kW]	50 - 240	140 - 180	100 - 200	100 - 300
# pulses, pulse length	8 x 8sec	19 x (2-8)sec	21 x (2-20)sec	21 x (5-20)sec
Total discharge time	~60s	~65s	~220s	~630s
(a) Recovered atoms (x10^{22})	1.6 H	2.9 H	6.2 D	-
(b) Retained atoms (x10^{22})	4.8 D	2.5 D	8.6 H	-
Ratio (b) to (a)	3.0	0.86	1.4	-

Table 1: Overview experimental conditions and particle balance for four JET ICWC isotopic exchange experiments, labelled I, II, III & IV. Analysis of exp. IV is ongoing.

	JET-C D_2-ICWC^{I}	JET-ILW D_2-ICWC^{II}	JET-ILW H_2-ICWC^{III}	JET-ILW D_2-ICWC^{IV}
Recovered atoms (%)	< 25%	> 67%	85%	*~ 100% (tbd)*
Accessible fuel reservoir	> 6.4e22	> 4.3e22	~7.3e22	*tbd*

Table 2: Estimation of the accessible fuel reservoir by ICWC on JET-C and JET-ILW. Analysis of exp. IV is ongoing (tbd = to be determined).

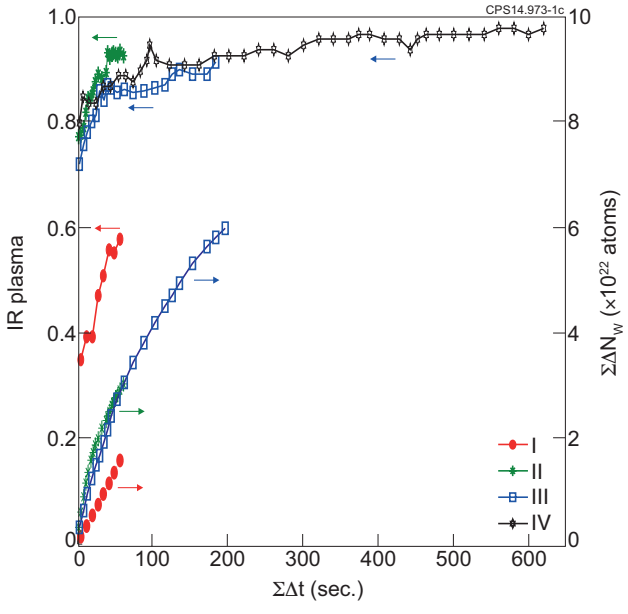

Figure 1: Isotopic exchange by ICWC as function of cumulated discharge time ($\Sigma\Delta t$) on JET-C^{I} and JET-ILW^{II,III,IV} (discharge parameters for labels I, II, III, IV are given in Table 1). Left axis: averaged plasma isotopic ratio (IR_{pl}) per discharge obtained from H and D beta radiation; Right axis: cumulated sum of the removed wall isotopes $\Sigma\Delta N_w$.

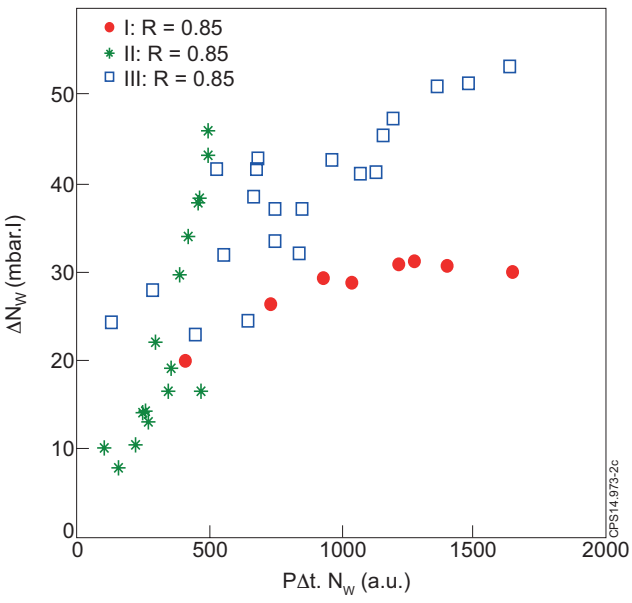

Figure 2: Removed amount of wall isotopes ΔN_w as function of coupled RF power P, pulse length Δt and remaining loaded wall isotope concentration Nw for ICWC isotopic exchange discharges on JET-C^{I} and JET-ILW^{II,III} (discharge parameters for labels I, II & III are given in Table 1, R is the correlation coefficient). [10]

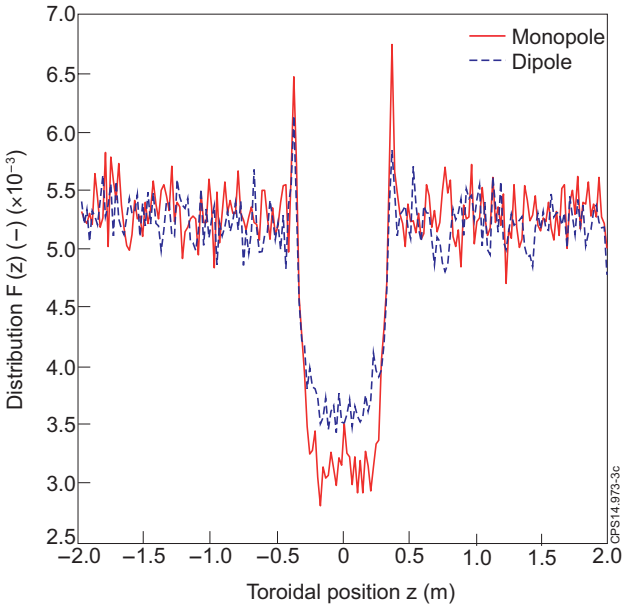

Figure 3: Toroidal distribution of ionization events for monopole and dipole simulated by Monte Carlo ICRF plasma breakdown code RFdinity1D [13].

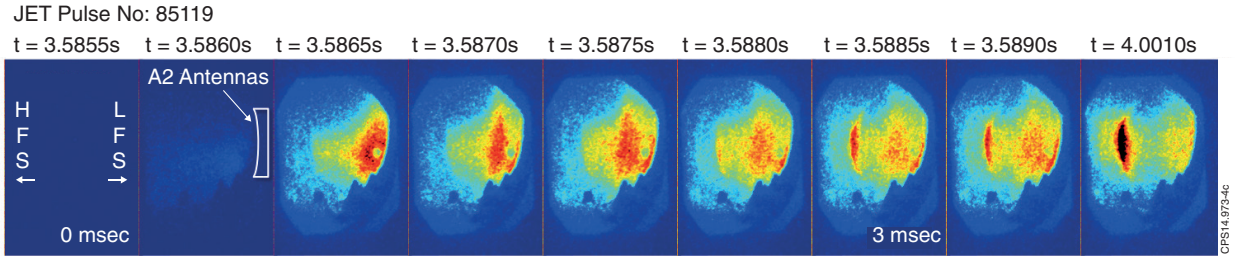

Figure 4: ICRF plasma production at JET. The discharge initiates at the low field side (LFS). Rapid radial expansion over 3 msec is driven by wave propagation.

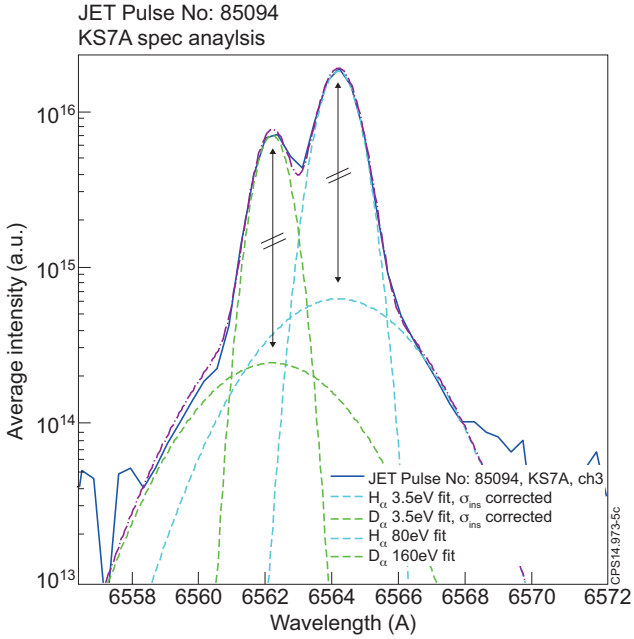

Figure 5: JET Pulse Number: 85094 Time average of H_α (~ 656.3nm) + D_α (656.1nm) spectrum over discharge duration. In addition to the main cold (3.5eV) contributions a warm component (80–160eV) is visible.